

# **GAS JOURNAL BEARING STABILITY VERSUS AMPLITUDE RATIO**

Florin Dimofte

The University of Toledo, currently working at NASA Lewis  
Research Center in Cleveland, Ohio,

Robert C. Hendricks,

NASA Lewis Research Center, Cleveland, Ohio, and

Theo G. Keith, Jr.

The University of Toledo, Toledo, Ohio.

## **ABSTRACT**

A gas journal bearing with a wavy surfaces was tested over a range of speeds up to 18,000 RPM to determine its stability in an unloaded condition as a function of the wave amplitude. The bearing was 50 mm in diameter, 58 mm long and had 0.0165 mm radial clearance. Three waves were created on the inner surface by deforming the bearing sleeve. The ratio of the wave amplitude to the radial clearance (the wave amplitude ratio) was varied from zero to 0.3.

It was found experimentally that for wave amplitude ratios equal to 0.187, or larger the bearing ran in a stable mode up to a critical speed after which it began to experience sub-synchronous whirl with a frequency close to one half the synchronous frequency. The speed threshold when the sub-synchronous whirl motion began was found to be a function of the wave amplitude ratio. For example, this threshold speed was 9,650 RPM for a wave amplitude ratio of 0.187 and 17,210 RPM for a wave amplitude ratio of 0.30. However, for wave amplitude ratios smaller than 0.187 (such as 0.024 and 0.157) the bearing became sensitive to sub-synchronous whirl motion at very low speeds. Moreover, it developed a super-synchronous whirling motion with a frequency close to twice the synchronous frequency. A wave amplitude ratio equals to 0.187 or greater than this suppressed both the sub- and super-synchronous whirl motion and allowed the bearing to run in a very stable mode. These experimental data was shown to be in good agreement with numerical predictions.

## **INTRODUCTION**

Fluid film bearings can experience stability problem such as a whirl motion of the shaft inside the bearing. The frequency of this motion is, in most cases, equal or less than one-half of the shaft frequency and is called "Sub-Synchronous Frequency Whirl," (SSFW). Unloaded plain journal bearings are very susceptible to SSFW. Gas plain journal bearings experiencing SSFW usually develop an unstable motion and wall contact generally occurs immediately after the onset of the whirl motion, due to the gas film low damping propriety, resulting in bearing failure. This phenomena was observed soon after gas bearings were applied starting in the middle 1950's. Due to its importance for bearing life SSFW was thoroughly analyzed as a fluid film instability condition. Among others, Castelli and Elrod [1] and Constantinescu [2] contributed work that theoretically established when SSFW occurs.

Unlike the plain journal bearing (Fig. 1a), a wave journal bearing reduces the susceptibility to SSFW. A wave journal bearing [3] is a bearing with a slight, but precise, variation in the circular profile of the bearing such that a waved profile is circumscribed on the inner bearing diameter. The profile has a wave amplitude that is a fraction of the bearing clearance. Figure 1b, shows a three-wave bearing. The clearance and the wave and the wave's amplitude are greatly exaggerated in Figs. 1a and 1b so that the

concept may be visualized.

The capacity of the wave journal bearing to reduce the susceptibility to SSFW was demonstrated theoretically in 1993 [3]. A parametric study over a broad range of bearing parameters indicated that the wave journal bearing offers better stability than the plain journal bearing for all operating conditions. However, the wave journal bearing's performance is dependent upon the wave amplitude and performance increases significantly as the wave amplitude increases.

Experimental work on gas wave journal bearings validated numerical predictions [4]. It was also demonstrated that an unloaded journal bearing with an altered circular profile, such as a wave bearing, allows operation over a range of speeds under which the bearing can run free of SSFW while the plane journal bearing is unstable. When the wave journal bearing develops SSFW the radius of this motion increases up to a size where the equilibrium between the radial force generated by the whirl movement and the pressure force in the film is established. This newly established equilibrium radius is smaller than the bearing clearance and the bearing can run in a stable manner.

The strong dependence of the wave bearing steady-state and dynamic performance upon the wave amplitude can be used as a tool to control the bearing behavior by changing the wave amplitude, [5]. The control of bearing dynamics by actively controlling the bearing surface profile was also reported [6]. It was shown that active bearing deflection control can be used to significantly reduce vibration in a machine.

The purpose of the present work is to provide correlation between the bearing dynamic behavior and wave amplitude. Therefore, a journal bearing (50 mm in diameter, 58 mm long, and 0.018 mm radial clearance) was used. The inner surface of the bearing sleeve can be waved to obtain a three wave bearing profile. Figure 2 shows that applying three forces ( $F$ ) on the outer diameter of the bearing sleeve at 120 degrees results in a three wave bearing profile due to the distortion of the bearing sleeve. The wave amplitude is a function of the magnitude of the force  $F$ . Various forces were applied in order to obtain wave amplitude over radial clearance ratios from zero to 0.3. The bearing profile was inspected each time after the wave amplitude was changed in order to assure the accuracy of the measurements.

This work was focused on the influence that the wave amplitude has on fluid film stability. Thus, the unloaded condition was selected because the maximum sensitivity of gas journal bearings to SSFW occurs when operated in this condition. The work was performed by using the wave journal bearing test rig at the NASA Lewis Research Center in Cleveland. The experimental results were compared to numerical predictions of the instability thresholds.

## TEST RIG

A bench test rig was assembled to provide information about how a journal bearing behaves when SSFW movement occurs [4]. The bearing tester uses a commercial spindle capable of 30,000 RPM with a run-out of less than 1 micron. The rig was set up with the shaft oriented vertically such that the test bearing could easily run in an unloaded condition (Fig. 3). Air at atmospheric conditions, was used as the lubricant. The test bearing is supported by double thrust levitation air bearing plates that allow the bearing to move very freely in the radial direction (Fig. 4). Two pairs of displacement sensors allow measurement of bearing orbits with respect to the shaft at two locations, just above and just below the test bearing. This configuration allows the bearing threshold susceptibility to SSFW to be precisely observed and provides information how the bearing behaves under SSFW.

## EXPERIMENTAL RESULTS

The test bearing has a mass of 5.2 kg. The various wave amplitude values of the test bearing were established by applying three equal forces, as shown in Fig. 2. The bearing profiles were measured each time the wave amplitude was changed in order to verify the shape of the waves and their uniformity around the circumference and along the bearing length. Thus, considering the bearing's vertical axis, two inspection planes were selected, each at approximately 1/3rd the bearing length from the top and bottom edges of the bearing. Figure 5 shows the measured bearing profiles in both selected inspection planes (marked TOP and BOTTOM). Both were displayed in the figure to distinguish any differences between them.

To observe the dynamic behavior of the bearing, proximity probes, shown in Fig. 4, were connected to two oscilloscopes. The screens of this two scopes are shown in Figs. 6 and 7. The bottom screen of each presents the orbit of the bearing with respect to the shaft by combining the signal from the two proximity probes placed at 90 degrees in the top (or the bottom) plane, (see Fig. 4). These signals control the X-Y channels of the scope. It should be noted: i) that the shaft is very stiff while the bearing is free to move in the radial direction, and ii) that each division of the bottom screen in Figs. 6 and 7 is approximately  $5\text{ }\mu\text{m}$ . The signal from one proximity probe is also connected to the next scope in order to visualize the vibration in one direction as well as to read the vibration frequency. The screen of this scope can be seen in the upper portion of each inset of Figs. 6 and 7. The output of the turning speed reader (measured in RPM) has been inserted between the upper and lower screens in Figs. 6 and 7.

### Tests of a circular bearing and a bearing with small impressed waves

First, the "true circular" bearing was considered when the applied forces were set at their minimum value in order to just keep the bearing sleeve in place. The profile of this "true circular" bearing was measured (Fig. 5a) and the maximum deviation from a true circle was found to be  $0.4\text{ }\mu\text{m}$ . This corresponds to a "wave amplitude ratio" (WAR) of 0.024. The next arrangement was for a bearing with a wave amplitude of  $2.5\text{ }\mu\text{m}$  which corresponds to a WAR of 0.157. The profiles of both bearings are shown in Figs. 5a and 5b. The wave profile shown in Fig. 5b is uniform in the circumferential direction and very small differences between top and bottom measurements can be observed.

Tests of both these bearing profiles reveal that SSFW motion is present from the beginning of the shaft rotation. At 680 RPM, as shown in Fig. 6, the bearing makes large orbits (lower screen) and the frequency of this motion is 5.594 Hz. This whirl frequency is very close to one half of the rotation (synchronous) frequency ( $680/60 = 11.33\text{ Hz}$ ,  $11.33/2 = 5.67\text{ Hz}$ ). If the bearings is locked, the whirling motion vanishes and the synchronous frequency (measured as 11.27 Hz, see Fig. 6b, upper screen) is predominant. In addition, the shape of the curve shown in the upper screen of Fig. 6b indicates that a vibration with a frequency equal to double of the synchronous frequency is superposed over the synchronous vibration. No explanation as to why this super-synchronous whirling motion is generated can be offered at time. However, this motion has a very small amplitude (the scale of the upper screen of Fig. 6b is  $0.5\text{ }\mu\text{m}$  per division in the vertical direction).

### Tests of bearings with wave amplitudes between 0.187 and 0.3.

Four cases were considered; the corresponding WAR's are 0.187, 0.22, 0.28, and 0.3. The profiles of two of these are shown in Figs. 5c and 5d for WAR's equal to 0.22 and 0.30, respectively. In Fig. 5c and 5d, the wave shape is uniform around the circumference of the bearing and the differences between the top and bottom profiles are negligible.

Tests of these cases indicate that the wave bearing can run in a perfectly stable mode up to a certain critical speed. The value of this speed is a function of the WAR, and was found to be 9,650, 13,788, 16,374, and 17,210 RPM for WAR's equal to 0.187, 0.22, 0.28 and 0.30, respectively.

A typical case is presented in Fig. 7 for a WAR equal to 0.22. The bearing was stable up to 13,788 RPM. The bearing behavior in the vicinity of the maximum stable speed was recorded and shown in Fig. 7a at 13,343 RPM. Thus, the bearing developed a dynamic orbit with a diameter of 5 to 6  $\mu\text{m}$  (see the lower screen of Fig. 7a). This motion is synchronous, and only synchronous at 222.2 Hz (see the upper screen of Fig. 7a). By increasing the speed and approaching 13,788 RPM, the SSFW begins to develop and is superposed over the synchronous motion. The upper screen of Fig. 7b shows that the period of the main vibration is now almost double than of the former synchronous vibration period and corresponds to a frequency of 114.3 Hz. The lower screen of Fig. 7b shows that the orbits are not more stable covering a larger area than in Fig. 7a, in a non-repetitive manner.

## FLUID FILM DYNAMIC STABILITY ANALYSIS

The geometry of a three wave bearing is shown in Fig. 8, where  $R$  is the shaft radius,  $C$  is the radial clearance,  $O$  is the center of the bearing,  $O_1$  is the center of the shaft,  $e$  the bearing eccentricity,  $e_w$  the wave amplitude (the distance between the wave's peak and the mean circle with the radius  $R + C$ ),  $W$  is the applied load, and  $F$  is the bearing's load capacity that is equal to the applied load at equilibrium.

In a bearing stability calculation, as a first approach, the rotor can be considered rigid and symmetrical, and supported by two identical bearings. Therefore, each bearing carries a mass  $M$  that is one-half of the rotor mass. The motion equation of the center of the shaft inside the bearing can be written as:

$$\begin{bmatrix} (Z_{xx} - M v^2) & Z_{xy} \\ Z_{yx} & (Z_{yy} - M v^2) \end{bmatrix} \begin{bmatrix} x \\ y \end{bmatrix} = 0$$

where the bearing is represented by its four impedance coefficients,  $Z_{jk} = K_{jk} + i v B_{jk}$  ( $j = x, y; k = x, y$ ).  $K_{jk}$  and  $B_{jk}$  are the bearing dynamic stiffness and damping coefficients when the bearing is whirling with the frequency  $v$ . These dynamic coefficients can be calculated by using a small perturbation technique [7].

The threshold of instability occurs when the determinant of the matrix is zero and the corresponding mass,  $M_c$ , is the mass required to develop the SSFW movement of the shaft inside the bearing. The bearing can run free of the half frequency whirl motion when its actual allocated mass is less than the critical mass ( $M_c$ ).

## COMPARISON OF EXPERIMENTAL DATA TO NUMERICAL PREDICTIONS

The above analysis has been used to predict the critical mass for the experimental bearing operating in an unloaded condition. WAR's from zero (true circular) to 0.35 were used. The results are plotted in Fig. 9 where it is seen that a true circular bearing is unstable for any bearing mass. In addition, a WAR equal to 0.15 will not allow the experimental bearing with a mass of 5.2 kg to run in a stable mode for any speed. The predicted curve for a WAR of 0.15 is below the actual bearing mass line at all speeds from zero to 30,000 RPM. This result is in complete agreement with the experiment data. The bearing with both almost zero and a 0.157 WAR manifest SSFW motion shortly after the shaft begins turning.

However, if the WAR is increased, a portion of the predicted curves lie above the bearing mass line. In these regions the bearing can run in a stable mode free of SSFW motion. For example, the

critical mass curve for a WAR equal to 0.2 crosses the actual bearing mass line at 10,000 RPM. This means that for speeds from zero to 10,000 RPM the bearing with a WAR equal to 0.2 should be stable, and when operated at speeds exceeding 10,000 RPM, it should experience SSFW motion.

The experimentally observed threshold to SSFW motion for a bearing with a WAR equal to 0.187, or larger is also plotted in Fig. 9 as a set of scattered points that are located on the horizontal line at the actual bearing mass value of 5.2 kg. Essentially, the intersection points of this line with the predicted critical mass curves indicate the predicted speeds at which a bearing with a mass of 5.2 kg begins SSFW motion for given WAR values. Figure 9 demonstrates that the experimental data points are in good agreement with predicted values.

## CONCLUSIONS

A gas journal bearing was tested over a range of speeds up to 18,000 RPM. The purpose of the tests was to determine bearing stability under an unloaded condition as a function of wave amplitude. The bearing was 50 mm in diameter, 58 mm long and had 0.0165 mm radial clearance. The inner surface of the sleeve was forced into a wave shape. Three waves were used. The wave amplitude over the radial clearance ratio was varied from zero to 0.3. The bearing profile was inspected after the wave amplitude was altered.

The conclusions of this work are:

1. Wave amplitude ratios equal to 0.187, or larger allow the bearing to run in a stable mode up to a critical speed at which it begins to experience sub-synchronous whirl with a frequency close to one half of the synchronous frequency.
2. The speed threshold when the sub-synchronous whirl motion begins is a function of the wave amplitude ratio. This threshold was found, for example, to be 9,650 RPM for a 0.187 wave amplitude ratio and 17,210 RPM for a 0.30 wave amplitude ratio.
3. Wave amplitude ratios smaller than 0.187 such as 0.157 or 0.024 resulted in the bearing becoming sensitive to sub-synchronous whirl motion from very low speeds. Moreover, the bearing develops a super-synchronous whirling motion with a frequency close to twice the synchronous frequency. A wave amplitude ratio equals to 0.187 or greater than this suppresses both the sub- and super-synchronous whirl motion and allows the bearing to run in a very stable mode.
4. The experimental results are in good agreement with numerical predictions.

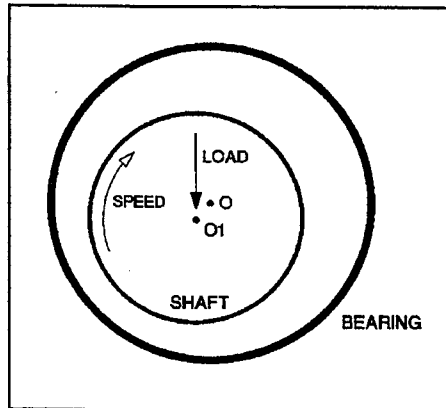
## ACKNOWLEDGMENTS

This paper reports work conducted at the NASA Lewis Research Center in Cleveland Ohio sponsored under grant NAG3-388 awarded to the University of Toledo. The authors would like to express their thanks to George Stefko from NASA LeRC who kindly supported this work.

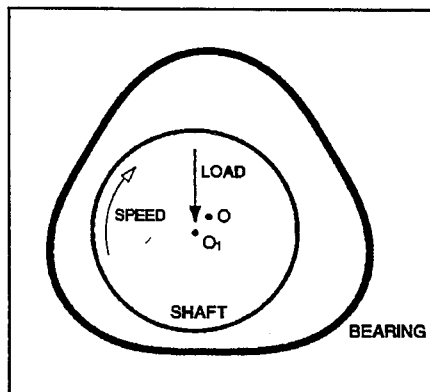
## REFERENCES

1. Castelli, V. and Elrod, H.G., "Solution of the Stability Problem for 360 Deg Self-Acting, Gas-Lubricated Bearings," *Journal of Basic Engineering*, Trans. ASME, Series D, Vol. 87, 1, pp. 199-212, (1965).

2. Constantinescu, V.N., "On Hydrodynamic Instability of Gas-lubricated Journal Bearings," *Journal of Basic Engineering*, Trans. ASME, Series D, Vol. 87, 3, pp. 579-588, (1965).
3. Dimofte, F., "Wave Journal Bearing with Compressible Lubricant; Part I: The Wave Bearing Concept and a Comparison with a Plain Circular Journal Bearing", presented to STLE 1993 Annual Meeting, May 17-20, 1993, Calgary, Canada, published in *STLE Tribology Transactions* Vol. 38 1, pp. 153-160, (1995).
4. Dimofte, F., and Hendricks, R.C., "Fractional Whirl Motion in Wave Journal Bearings" presented at The Fourth Seal Code Development Workshop held at NASA Lewis Research Center in Cleveland, Ohio, on June 14-15, 1995, NASA CP 10181, pp. 337-340.
5. Dimofte, F "A Waved Journal Bearing Concept - Evaluating Steady-State and Dynamic Performance with a Potential Active Control Alternative", Proceedings of the ASME 14th Biennial Conference. on Mechanical Vibration and Noise, September 19-22, 1993, Albuquerque, NM, DE-Vol. 60, Vibration of Rotating Systems, pp. 121-128.
6. Rylander, H.G., Carison, M.J.T., and Lin, C.R., "Actively Controlled Bearing Surface Profiles, Theory and Experiments" published in Proceedings of The Energy and Environmental Expo '95 - The Energy-Sources Technology Conference and Exhibition held in Houston, Texas January 29 - February 1, 1995, PD-Vol. 72, Tribology Symposium, pp. 11-14, ASME 1995.
7. Dimofte, F., "Effect of Fluid Compressibility on Journal Bearing Performance," *STLE Tribology Transactions* Vol. 36, 3, pp. 341-350, (1993).



a. True Circular,



b. Three Wave,  
Fig. 1 Journal Bearings.

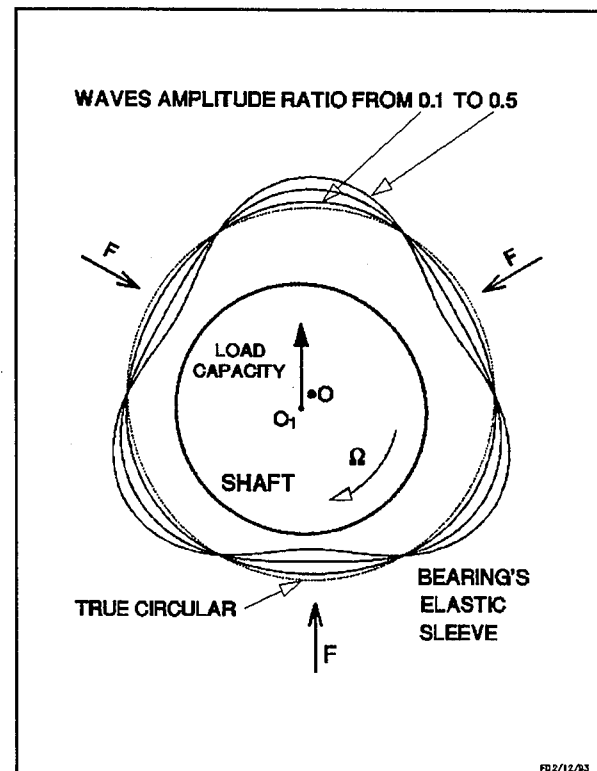


Fig. 2 Wave Bearing with Various Wave Amplitudes.

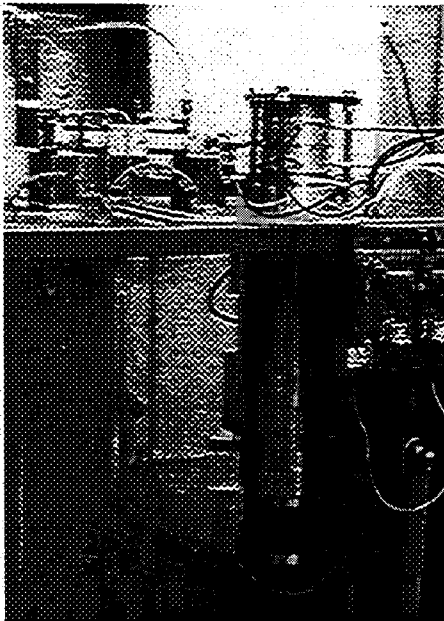
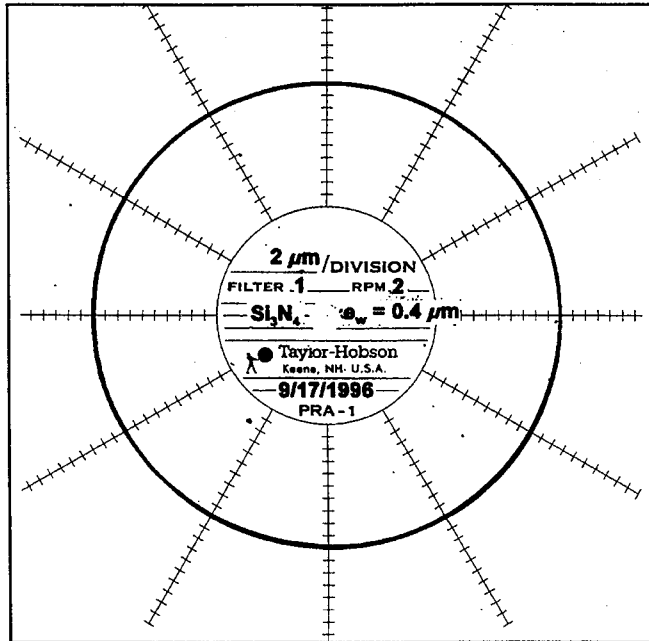


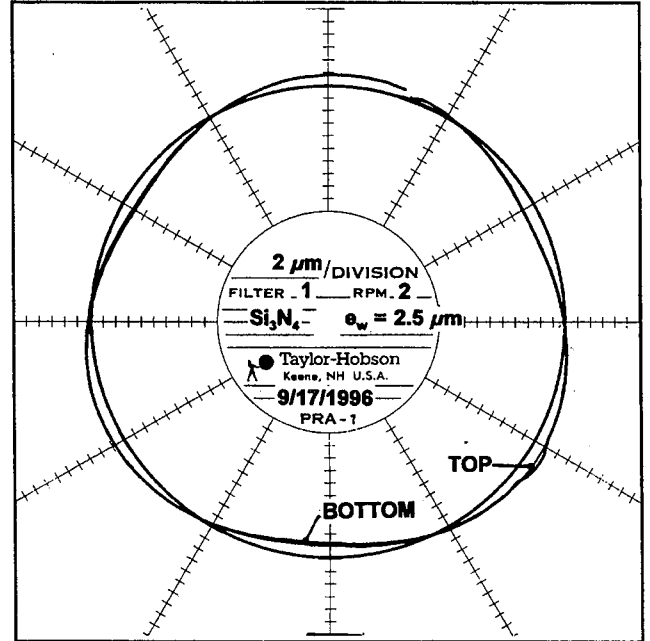
Fig. 3 Test Rig



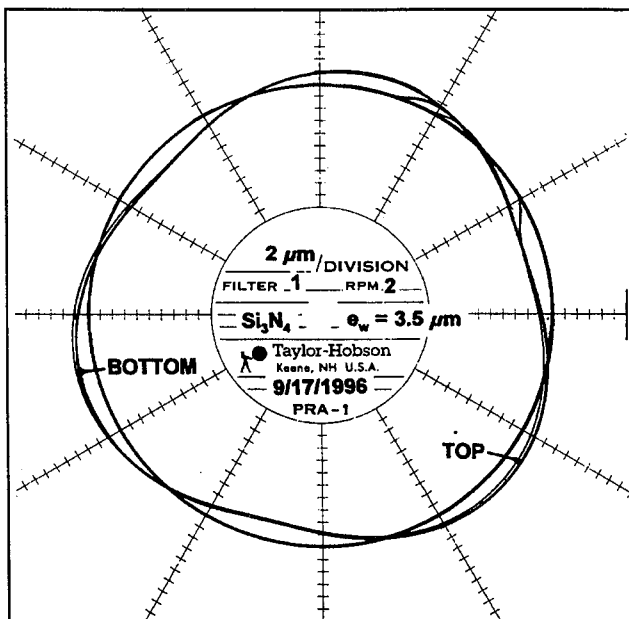
Fig. 4 Experimental Bearing for Sub-Synchronous Frequency Whirl Test



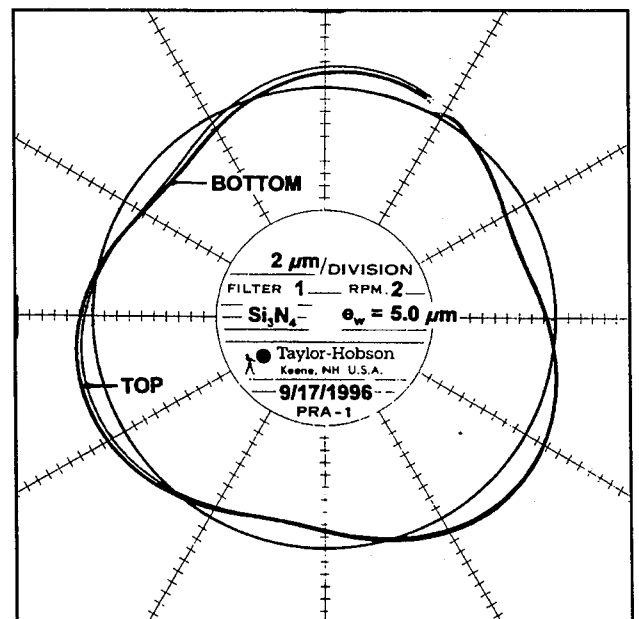
a. "True Circular", WAR = 0.024



b. WAR = 0.157



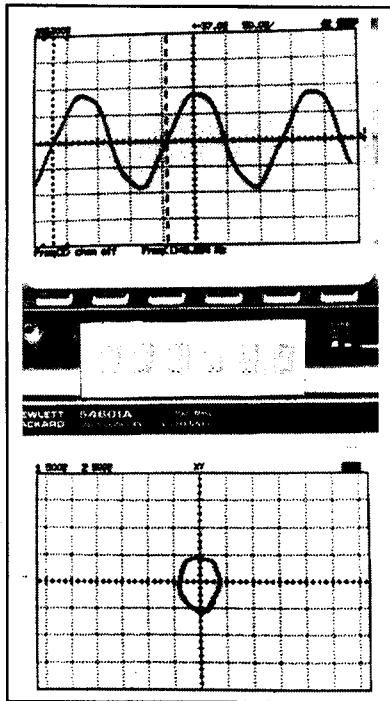
c. WAR = 0.22



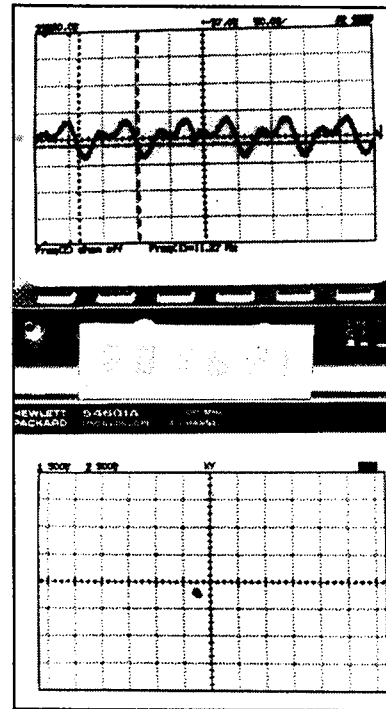
d. WAR = 0.30

Fig. 5 Test Bearing Profiles



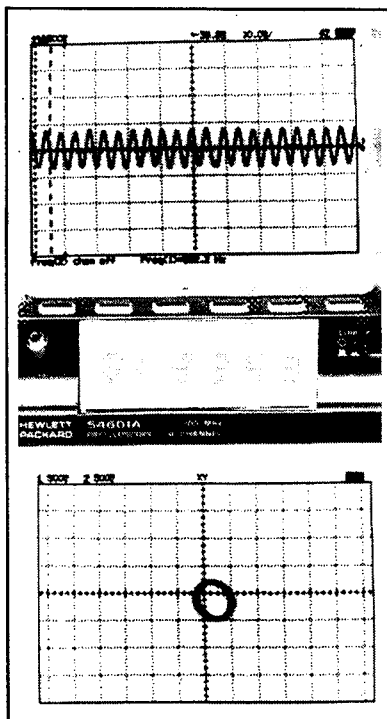


**a. Sub-Synchronous Whirl, Free Bearing**  
Speed = 680 RPM, Whirl Frequency = 5.6 Hz

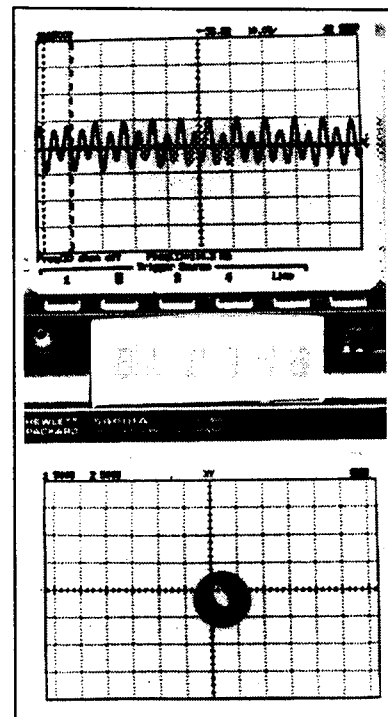


**b. Synchronous and Super-Synchronous Whirl,**  
Locked Bearing, Speed = 681 RPM, Whirl  
Frequency = 11,27 and 22.54 Hz.

**Fig. 6 Unloaded Journal Bearing Behavior when WAR = 0.024 or 0.157**



**a. Synchronous Whirl (222.2 Hz)**  
at 13,343 RPM



**b. Start of Sub-Synchronous Whirling**  
(114.3 Hz) at 13,788 RPM

**Fig. 7 Unloaded Journal Bearing Behavior when WAR = 0.22**

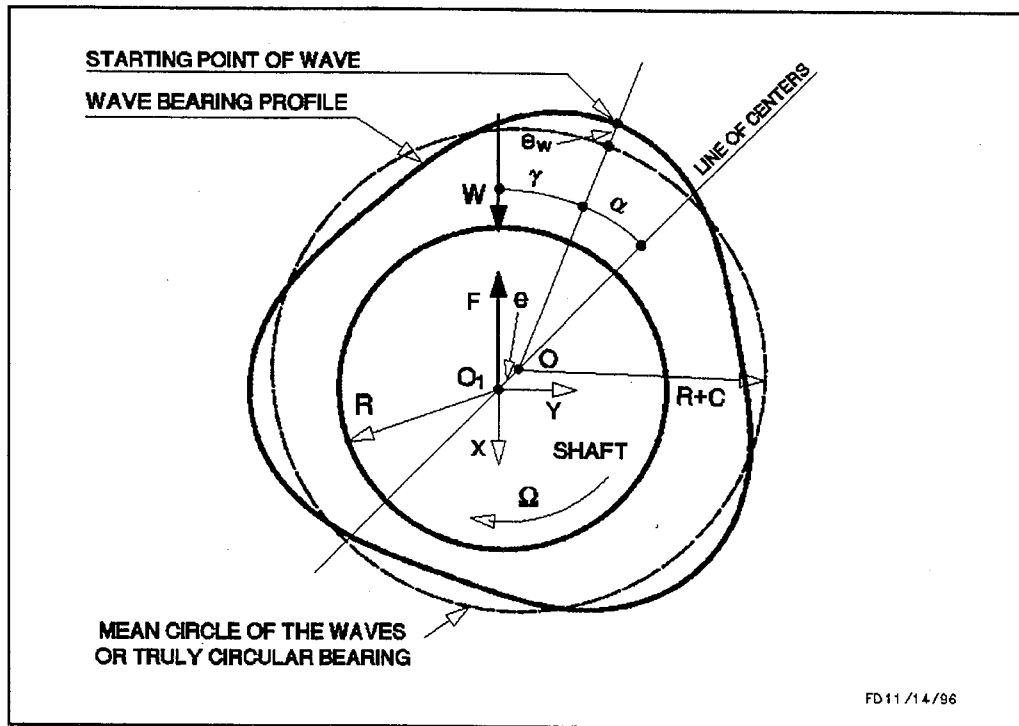


Fig. 8 Three Wave Journal Bearing Geometry

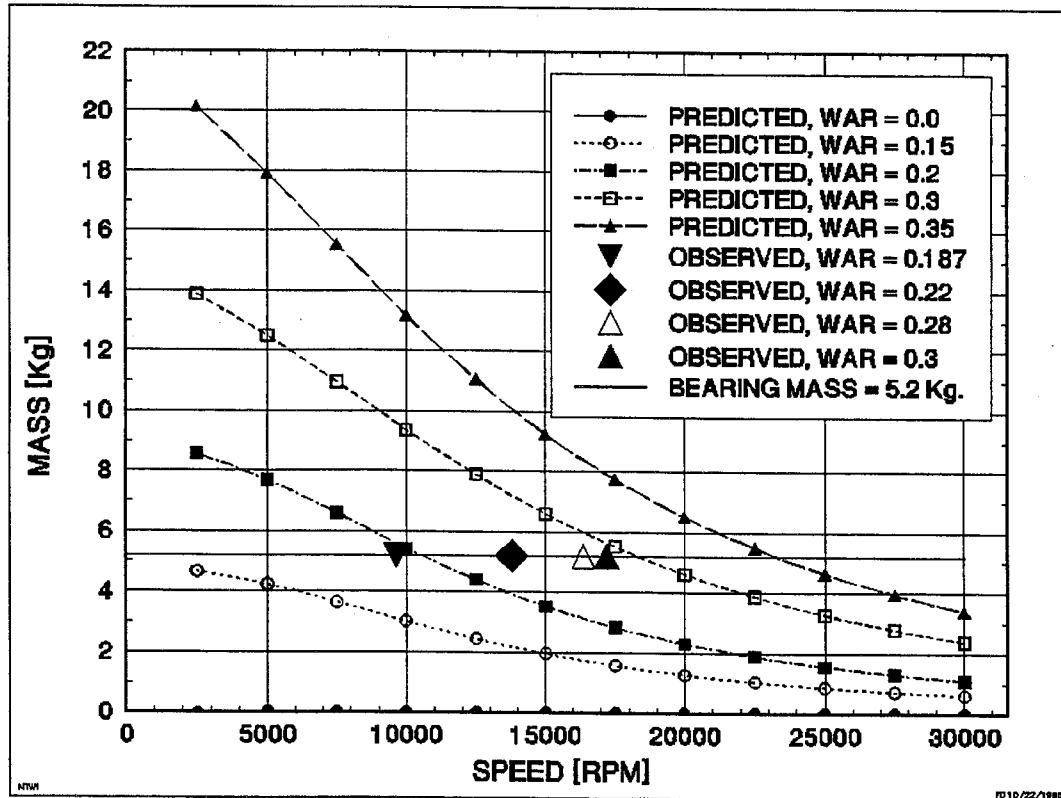


Fig. 9 Predicted Critical Mass and Experimentally Observed Threshold of Whirling.